Electrocrystallization of Epitaxial Zinc Oxide onto Gallium Nitride

Th. Pauporté,*,† R. Cortès,‡ M. Froment,‡ B. Beaumont,§ and D. Lincot†

Laboratoire d'Electrochimie et de Chimie Analytique, Unité Mixte de Recherche-CNRS 7575, École Nationale Supérieure de Chimie de Paris, 11 rue Pierre et Marie Curie, 75231 Paris Cedex 05, France, Physique des Liquides et Electrochimie, UPR 15 CNRS, Université P. et M. Curie, 75252 Paris, Cedex 05, France, and Centre de Recherche sur l'Hétéroépitaxie et ses Applications, Rue B. Gregory, Parc Sophia Antipolis, 06560 Valbonne, France

Received May 1, 2002. Revised Manuscript Received September 3, 2002

We have studied in detail the structure and the nucleation and growth process of electrodeposited epitaxial hexagonal ZnO on GaN(0001). The crystallites grow with the *c*-axis perpendicular to substrate and the in-plane relationship is ZnO[100] || GaN[100]. We show that the deposit aspect progressively changes with the deposition time from isolated dispersed dots toward fully covering flat zinc oxide single crystals. A simple model is presented which explains these morphological changes. The nucleation is instantaneous and the growth rate is controlled by the crystal surface reactions. The velocity of crystal growth is found dependent on the crystallographic face of the grain: it is approximately five times faster on the {0001} planes than on the $\{10\bar{1}0\}$ and $\{01\bar{1}0\}$ families of planes. We show that nucleation problems are encountered with high-quality GaN presenting a low surface defect density. The difficulty has been overcome by chemically treating the substrate with an aqueous ammonium hydroxide solution prior to the deposition. This treatment allows the nucleation of zinc oxide but has a detrimental effect on the deposit "mosaicity" which is better in the case of GaN with high defect density.

Introduction

Recently, zinc oxide has emerged as an interesting candidate for blue light emitting devices such as light emitting diodes and laser diodes. ZnO has a wide band gap of 3.3 eV which can be tuned from 2.8 to 4.0 eV by alloying with CdO or MgO.[1] It presents some interesting optoelectronic features in view of these applications, for example such as a large exciton energy (60 meV)[2] and a low power threshold for optical pumping at room temperature.[3] Recently, the preparation of p-type ZnO has attracted much attention.[4,5]

Electrodeposition has emerged as an interesting soft, low-temperature route for the preparation of high-quality epitaxial films of binary chalcogenides[6−13] or oxides[14−22] and we have recently reported[21] the successful epitaxial growth of zinc oxide single crystal on gallium nitride (0001) by this method. Both film and substrate have a würtzite hexagonal structure. At room temperature, the *a* lattice parameter of bulk GaN ranges from 3.160 to 3.190 Å and the parameter *c* ranges from 5.125 to 5.190 Å.[23] For bulk ZnO, *a* is reported to range from 3.249 to 3.253 Å and *c* from 5.206

* To whom correspondence should be addressed.
† Laboratoire d'Electrochimie et de Chimie Analytique.
‡ Physique des Liquides et Electrochimie.
§ Centre de Recherche sur l'Hétéroépitaxie et ses Applications.

(1) Ohtomo, A.; Kawasaki, K.; Koida, T.; Koinuma, H.; Sakurai, Y.; Yoshida, Y.; Sumiya, M.; Fuke, S.; Yasuka, T.; Segawa, Y. *Mater. Sci. Forum* **1998**, *264*, 1463.
(2) Hvam, J. M. *Solid State Commun.* **1978**, *26*, 987.
(3) Bagnall, D. M.; Chen, Y. F.; Zhu, Z.; Yao, T.; Koyama, S.; Shen, M. Y.; Goto T. *Appl. Phys. Lett.* **1997**, *70*, 2230.
(4) Joseph, M.; Tabata, H.; Kawai, T. *Jpn. J. Appl. Phys.* **1999**, *38*, L1205.
(5) Ryu, Y. R.; Zhu, S.; Look, D. C.; Wrobel, J. M.; Jeong, H. M.; White, H. W. *J. Cryst. Growth* **2000**, *216*, 330.
(6) Lincot, D.; Kampmann, A.; Mokili, B.; Vedel, J.; Cortes, R.; Froment, M. *Appl. Phys. Lett.* **1995**, *67*, 2355.
(7) Lincot, D.; Furlong, M.; Froment, M.; Bernard, M. C.; Cortes, R. *Mater. Res. Soc. Symp. Proc.* **1997**, *451*, 223.
(8) Furlong, M. J.; Lincot, D.; Froment, M.; Cortes, R. *Proc. − Electrochem. Soc.* **1997**, *27*, 106−113.
(9) Cachet, H.; Cortes, R.; Froment, M.; Maurin, G. *J. Solid State Electrochem.* **1997**, *1*, 100.
(10) Beaunier, L.; Cachet, H.; Froment, M.; Maurin, G. *J. Electrochem. Soc.* **2000**, *147*, 1835.
(11) Cachet, H.; Cortes, R.; Froment, M.; Etcheberry, A. *Thin Solid Films* **2000**, *361−362*, 84.
(12) Vertegel, A. A.; Shumsky, M. G.; Switzer, J. A. *Angew. Chem., Int. Ed.* **1999**, *38*, 3169.
(13) Beaunier, L.; Cachet, H.; Cortès, R.; Froment, M. *Electrochem. Commun.* **2000**, *2*, 508.
(14) Switzer, J. A.; Shumsky, M. G.; Bohannan, E. W. *Science* **1999**, *284*, 27.
(15) Bohannan, E. W.; Jaynes, C. C.; Shumsky, M. G.; Barton, J. K.; Switzer, J. A. *Solid State Ionics* **2000**, *131*, 97.
(16) Bohannan, E. W.; Shumsky, M. G.; Switzer, J. A. *Chem. Mater.* **1999**, *11*, 2289.
(17) Barton, J. K.; Vertegel, A. A.; Bohannan, E. W.; Switzer, J. A. *Chem. Mater.* **2001**, *13*, 952.
(18) Vertegel, A. A.; Shumsky, M. G.; Switzer, J. A. *Chem. Mater.* **2000**, *3*, 596.
(19) Nikiforov, M. P.; Vertegel, A. A.; Shumsky, M. G.; Switzer, J. A. *Chem. Mater.* **2000**, *12*, 1351.
(20) Vertegel, A. A.; Shumsky, M. G.; Switzer, J. A. *Electrochim. Acta* **2000**, *45*, 3233.
(21) Pauporté, T.; Lincot, D. *Appl. Phys. Lett.* **1999**, *75*, 3817.
(22) Liu, R.; Vertegel, A. A.; Bohannan, E. W.; Sorenson, T. A.; Switzer, J. A. *Chem. Mater.* **2001**, *13*, 508.
(23) Mandelung, O. *Semiconductors - Basic Data*; Springer: Berlin, 1996.

10.1021/cm020349g CCC: $22.00
Published on Web 10/08/2002

to 5.213 Å.[23] The average lattice mismatch defined as $(a_{ZnO} - a_{GaN})/a_{GaN}$ is thus as low as 2.4% and the GaN substrate lattice can be easily accommodated by the ZnO layer. After thermal annealing, the deposits exhibited well-defined photoluminescence properties accompanied by a band gap energy shifted toward a lower energy.[21]

The overall cathodic electrodeposition reaction for zinc oxide from a molecular oxygen precursor has been described as follows:[21,24−26]

$$Zn^{2+} + \frac{1}{2}O_2 + 2e^- \rightleftharpoons ZnO \qquad (1)$$

The first step is the electrogeneration of hydroxide ions from molecular oxygen reduction,

$$\frac{1}{2}O_2 + H_2O + 2e^- \rightleftharpoons 2OH^- \qquad (1a)$$

followed by the electroprecipitation of zinc oxide from the zinc ion dissolved in solution

$$Zn^{2+} + 2OH^- \rightleftharpoons ZnO + H_2O \qquad (1b)$$

In the present paper, we report on a detailed study of the structure of epitaxial ZnO deposits and of the nucleation and growth mechanism onto GaN. A simple model is presented which explains the morphological changes observed with the deposition time. We show that the deposit aspect progressively changes from isolated dispersed dots toward fully covering flat zinc oxide single crystals. We also report on nucleation features encountered with high-quality GaN and show that this difficulty can be overcome by chemically treating the substrate prior to deposition.

Experimental Section

The substrates were 1.3-μm-thick n-type GaN(0001) single-crystal layers deposited by metal organic vapor phase epitaxy (MOVPE) onto sapphire (0001) single-crystal wafers.[27] Two qualities of GaN have been used. A first set (noted A-GaN) presented a threading dislocation density of 100 μm^{-2} and was used in our previous work.[21] The second (noted B-GaN) was high-quality GaN with a dislocation density of 1 μm^{-2}. We used an etching process which consisted of dipping the GaN surface into a solution of 28% NH_4OH maintained at 50 °C for various time durations. The substrates were subsequently thoroughly rinsed in milliQ-quality filtered water (18.2 MΩ), dried under an argon stream, and mounted as an electrode. The electrical contact was made on the GaN by means of a Ga−In eutectic dot. The electrode surface in contact with the solution was delimited with an electroplating tape (3M). The surface area of the electrode ranged between 0.08 and 0.125 cm^{-2}.

The electrolytic solution contained 5 mM of reagent grade $ZnCl_2$ (Prolabo) and 0.1 M of reagent grade KCl (Prolabo) as the supporting electrolyte. An oxygen/ argon gas mixture was bubbled into the deposition bath. The oxygen concentration, fixed by the flow ratio between these two gases, is expressed as a percentage. At a constant applied potential, the growth rate is expected to be proportional to the oxygen concentration in solution.

The ZnO depositions were carried out at −1.4 and −1.5 V in a classical three-electrode cell. They were performed with a PAR 273A potentiostat from EG&G. All the potentials are referred to the saturated mercurous sulfate electrode (MSE with a potential of +0.65 V versus the normal hydrogen electrode (NHE)). The counter electrode was a platinum wire. The deposition bath temperature was set at 80 °C with a thermostat. The working electrode was fixed vertically, and the deposition bath was stirred by a magnetic stirring bar at 100 rotations per minute.

The morphologies of the films were studied with a Stereoscan 440 scanning electron microscope from Leica. The epitaxial growth of the films has been studied by reflection high-energy electron diffraction (RHEED) observations. A quantitative determination of the structure and the epitaxial orientation of the film was achieved by X-ray diffraction method, using a five circle goniometer especially designed for a thin film study.[28] In this device, the incident beam is at a glancing angle (ca. 0.6°) and the detector is positioned at a 2θ angle corresponding to a Bragg diffraction angle characteristic of the deposit. A cross section of a film deposited at −1.4 V onto a fluorine-doped SnO_2-covered Si wafer was prepared by mechanical grinning followed by ion milling, and studied by high-resolution transmission electron microscopy HRTEM (Philips CM 20, 200 keV).

Results

In Figure 1 are presented some scanning electron microscopy (SEM) top views of different epitaxial ZnO deposits. In Figure 1a−c, the A−GaN substrates were simply rinsed in acetone and pure water prior to the deposition experiment. The crystallites present a nanopillar hexagonal shape and are regular. Their surface coverage progressively increases from (a) to (c) with the deposition time, t_d. As already described in a previous paper,[21] the different crystallites exhibit parallel facets due to the in-plane epitaxial relationship.

The crystallites are very homogeneous in size. This shows that the nucleation of ZnO growth centers is very fast. In Figure 1b,c the crystallite density is measured equal to 9 μm^{-2}. Generally, "instantaneous" nucleation takes place on specific nucleation centers at the surface. This value is lower than the value of defect density, 100 μm^{-2}, which means that these defects are not involved in the nucleation or that only 9% of them are effective. The deposition time was longer with sample c than with sample b and a lot of merged grains are observed. This stage corresponds to the onset of the coalescence process. The epitaxial growth is maintained after full coalescence and appears not to be limited by the layer thickness. We can state that the ordered structure is maintained by the homoepitaxial growth of ZnO.

With the higher quality B-GaN, no film formation was observed with the same cleaning procedure of the substrate and growth conditions. This observation emphasizes the key role of GaN surface defects on the formation of epitaxial nucleation centers on A-GaN. We have tested different chemical etchings of B-GaN and found that a treatment in hot ammonia was efficient in promoting the growth of ZnO. An optimum etching duration has been found ranging between 20 and 35 min. The aspect of the GaN surface observed by SEM is similar before and after the ammonia treatment and no pitting is observed. Accordingly, the surface modification is most likely chemical.

(24) Peulon, S.; Lincot, D. *Adv. Mater.* **1996**, *8*, 166.
(25) Peulon, S.; Lincot, D. *J. Electrochem. Soc.* **1998**, *145*, 864.
(26) Pauporté, T.; Lincot, D. *Electrochim. Acta* **2000**, *45*, 3345.
(27) Xin, Y.; Pennycook, S. J.; Nellist, N. D.; Sivananthan, S.; Omnès, F.; Beaumont, B.; Faurie, J. P.; Gibart, P. *Appl. Phys. Lett.* **1998**, *72*, 2680.
(28) Froment, M.; Bernard, M. C.; Cortes, R.; Mokili, B.; Lincot, D. *J. Electrochem. Soc.* **1995**, *142*, 2642.

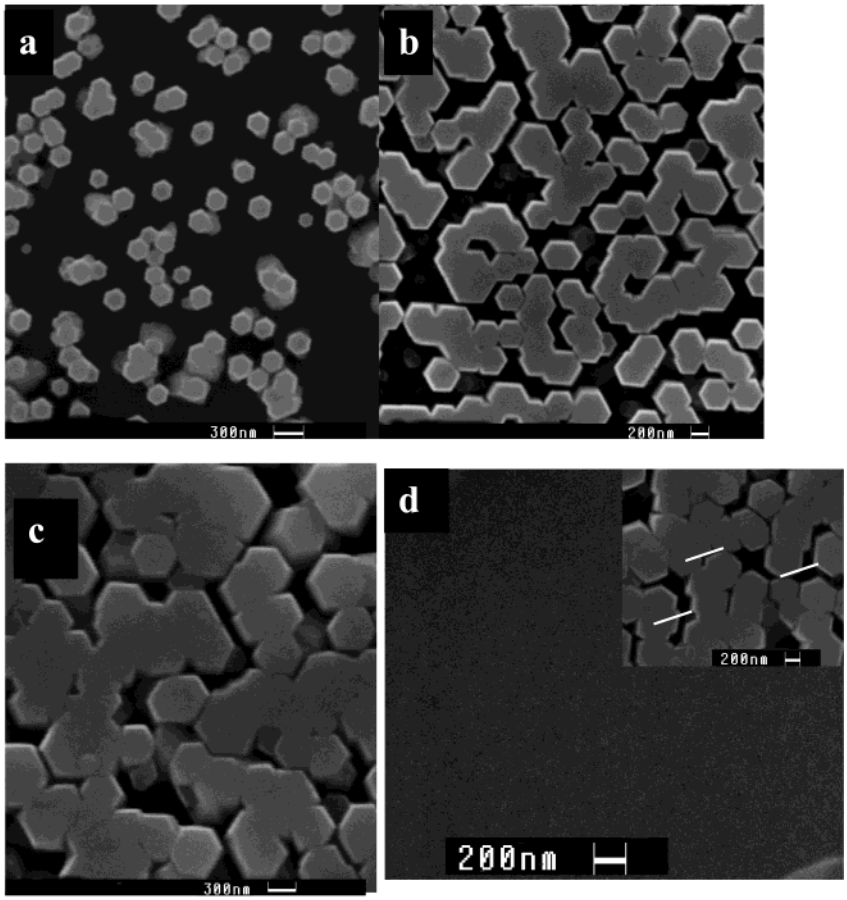

Figure 1. Top scanning electron micrographs of epitaxial ZnO. Deposition conditions: (a) A-GaN substrate, $t_d = 1100$ s, $E_d = -1.4$ V, 52% O_2; (b) A-GaN, $t_d = 4080$ s, $E_d = -1.4$ V, 27% O_2; (c) A-GaN, $t_d = 7000$ s, $E_d = -1.4$ V, 27% O_2; and (d) B-GaN etched 35 min in ammonia, $t_d = 1625$ s, $E_d = -1.5$ V, 65% O_2, (inset) same conditions, aspect before complete merging.

Figure 1d presents a 0.5-μm thick film deposited onto B-GaN etched 35 min. in hot ammonia prior to the deposition experiment. The deposition time was 30 min. The film fully covers the substrate and is flat. No grain boundary is observed and the core layer looks like a unique single crystal. The aspect of the layer before complete merging (inset) shows that the previous film results in the coalescence of the hexagonal grains. The epitaxy is proven by the alignment of the grain facets, which is exemplified by different lines drawn in the inset figure.

Figure 2 shows the variation of the current densities as a function of the deposition time, t_d, recorded during the deposition of the films displayed in Figure 1c and d. The current density rapidly reaches a steady-state value in the case of A-GaN, whereas its increase is slower in the case of B-GaN. The currents recorded on GaN substrates are noisy compared to that on fluorine-doped SnO_2. The higher current density in curve b is attributed to both the higher oxygen concentration and the higher negative potential because the steady state current is not fully proportional to the oxygen concentration. Figure 2 shows that the epitaxial growth can be achieved over a large current density range.

The epitaxial growth has been characterized by the RHEED technique (Figures 3 and 4). Two different specific azimuths, $\langle 0\bar{1}0 \rangle$ (Figure 3) and $\langle 1\bar{1}0 \rangle$ (Figure 4) have been investigated. The spot pattern reveals that the film is epitaxially grown. Figures 3b and 4b represent the dot patterns expected for a hexagonal compact structure and show that the experimental data can be indexed with this structure. The following parameters values, $a = 0.325$ nm and $c = 0.521$ nm, are determined from the RHEED patterns and fit well with the expected values for ZnO. The spots are narrow in width revealing that the deposit is very well oriented with a low in-plane dispersion. They are also elongated along the growth direction, showing that the film is very flat as also

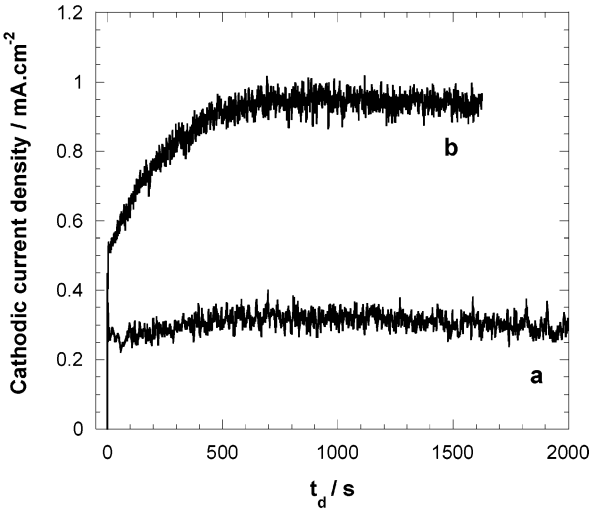

Figure 2. Current transients. (a) Same deposition conditions as in Figure 1c; (b) same conditions as in Figure 1d.

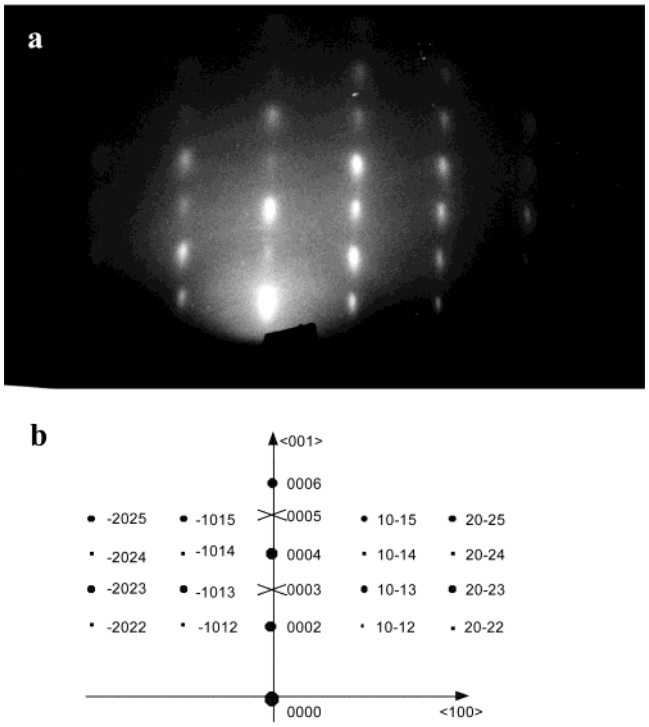

Figure 3. RHEED pattern of the film presented in Figure 1d observed under the $\langle 0\bar{1}0 \rangle$ azimuth (a) and indexation diagram with the hexagonal compact structure (b).

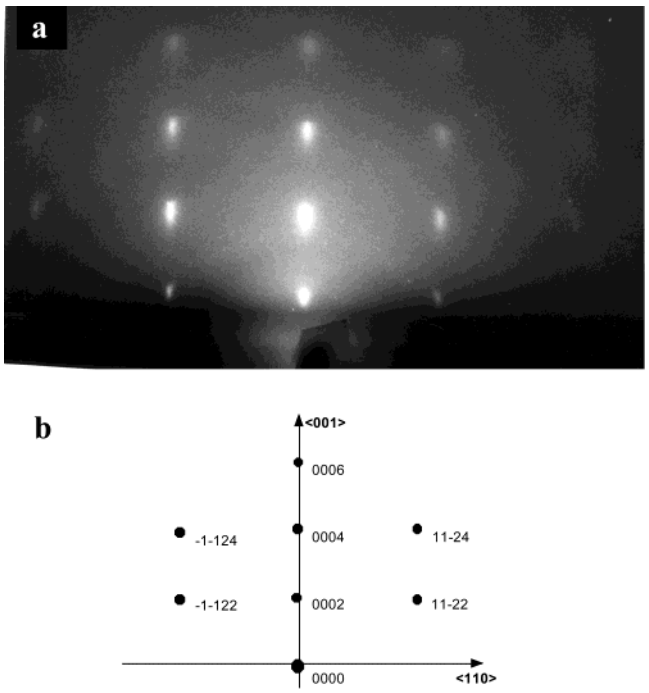

Figure 4. Same as Figure 3, $\langle 1\bar{1}0 \rangle$ azimuth (a) and indexation diagram (b).

observed by SEM (Figure 1d) and in our previous results.[21] The forbidden reflections (000*n*), with *n* an uneven integer, are observed with low intensities.

Figure 5a presents a GA-XRD spectrum of a 0.5-μm thick film deposited on a B-GaN treated 20 min in NH_4-OH (noted S2). The six peaks observed during a 360° Ψ (i.e., around an axis normal to the sample surface) scan is ascribed to the {101} plane family of GaN substrate. Figure 5b presents an enlarged view of peak bottom. It

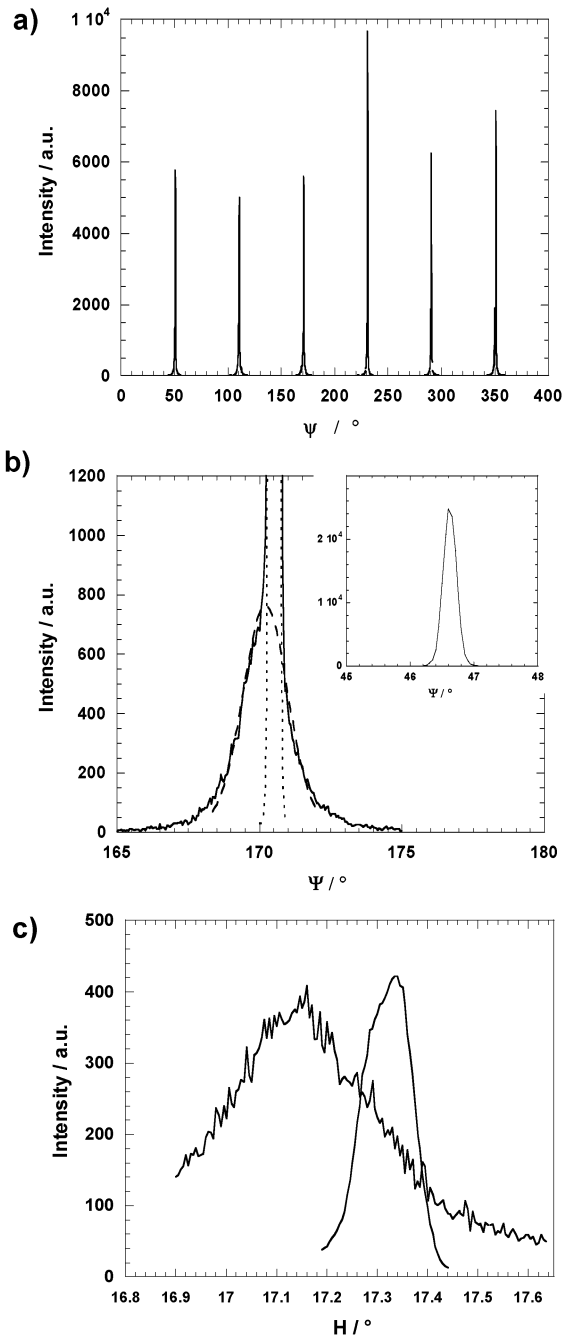

Figure 5. GA-XRD diagram observed at a glazing angle of 0.6° and a detector height of 17.06°: (a) Ψ scan of the {10$\bar{1}$1} family of planes; (b) enlarged view of a peak bottom (solid line), fit of GaN peak (dotted line) and of ZnO (dashed line) (Inset: same peak for bare GaN); (c) H scan of the (10$\bar{1}$1) ZnO peak (on the left) and of the GaN peak (on the right).

exhibits a dissymmetry with a shoulder on the left-hand not encountered with bare GaN (Figure 5b, inset). This is due to the presence of an additional peak, larger in width, ascribed to zinc oxide. Accordingly, the in-plane epitaxial relationship of the heterostructure is ZnO[100] || GaN[100]. The two peaks have been deconvoluted into the sum of two Gaussians which are reported on the same figure. The baseline is almost zero and reveals that the fraction of polycrystalline ZnO is negligible. The full width at half-maximum (fwhm) of ZnO and GaN have been determined for several samples prepared in different conditions and the results are summarized in

Table 1. Structural Parameters of Epitaxial ZnO Films Determined from GA-XRD Measurements at a Glancing Angle of 0.6°

sample	substrate	deposition potential (V vs MSE)	etching time (min)	oxygen conc. (%)	thickness (μm)	fwhm ZnO	fwhm GaN	texture
S1	B-GaN	−1.5	20	100	0.5	1.63	0.28	
S2	B-GaN	−1.5	36	65	0.5	1.91	0.25	0.58
S3	A-GaN	−1.4	0	25	1.1	0.74	0.47	0.60

Table 1. The better crystallographic quality of the B-GaN is confirmed with a fwhm of 0.25−0.28° instead of 0.47° for the A-GaN. The mean value of the ZnO peak fwhm measured on the six peaks of sample S1 is equal to 1.63°. Similarly, a mean fwhm equal to 1.91° is found with the sample S2. S1 and S2 films are of similar thickness, but in the latter case the substrate was treated during 36 min. instead of 20 min. We have previously reported[21] a fwhm equal to 0.74° with a 1.1-μm thick film grown on un-etched A-GaN (sample S3). As a consequence, it seems that if the ammonia treatment is necessary to obtained a good zinc oxide nucleation onto high-quality GaN, it may have a detrimental effect on the mosaicity of the deposit. By mosaicity, we mean that all the hexagonal grains do not have exactly the same orientation in the plane, and the fwhm of the Ψ scan reflects this dispersion. In contrast, the comparison of S1 and S3 shows that the mosaicity is not markedly influenced by the film thickness. Similarly, S1 and S2 reveal no significant influence of the oxygen concentration (growing rate) on the in-plane misorientation.

Figure 5c shows a detector height scan (H scan) of the sample S2. The incident angle was fixed at 0.6° and the azimuthal angle at 170.52° for GaN and 170.22° for ZnO. The narrower peak (0.12° fwhm) corresponds to the GaN and is slightly shifted compared to the broader one (0.34° fwhm) ascribed to ZnO. The texture, defined as the fwhm of an α scan, with α the angle between the ZnO crystallite *c*-axis and the direction perpendicular to the GaN surface, is calculated from the fwhm of the H scan. In the present conditions the $dH/d\alpha$ ratio is equal to 0.586. The results are summarized in Table 1 with no marked influence of the GaN substrate quality.

The internal structure of an electrodeposited ZnO grain has been observed by HRTEM (Figure 6). Each crystallite observed on SEM images (Figure 1b,c) corresponds to a single crystal. In Figure 6, the parallel lines, which are present throughout the micrograph, correspond to the (0002) lattice planes which are separated by a distance of 0.26 nm. We can observe that the film presents an excellent internal structure with no stacking faults.

Discussion

The nucleation growth mechanism can be easily studied in detail with epitaxial ZnO films on A-GaN for two principal reasons: the density of nucleation center is low, and the crystallized grains present sharp regular well-defined edges corresponding to the basic crystallographic planes. Consequently, the growth center density and the lateral and the vertical growth rates were easily determined from SEM top and cross-sectional views.

Figure 7 schematically displays a three-dimensional view of the GaN surface with ZnO growth centers. The

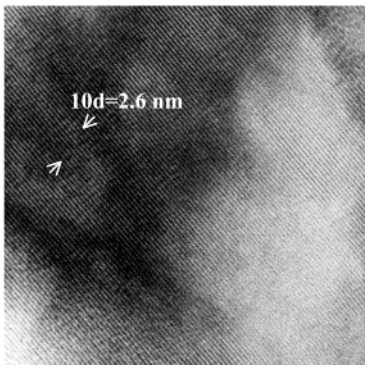

Figure 6. HRTEM image of a ZnO grain cross section.

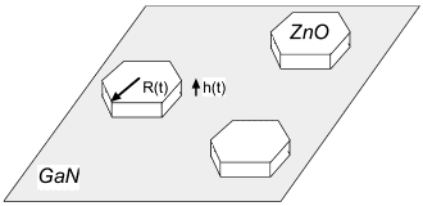

Figure 7. Schematic representation of the hexagonal ZnO growth center on GaN single-crystal substrate (N. B. the scale is arbitrary).

scale is arbitrary. During the first stage of deposit formation, the growth is three-dimensional. We note $R(t_d)$, the lateral facet length, and $h(t_d)$, the grain thickness, while *a* and *b* are the lateral and the vertical growth rates, respectively. These latter values have been calculated from the SEM views of films deposited during different deposition times. We have found that they are independent of t_d. Shortly after potential application, the nuclei are growing independently, but as the lateral growth proceeds, the adjacent center will come into contact and the different crystallites will merge. The Avrami Theorem relates the surface coverage of the film as a function of the extended area, S_e, defined as the notional area which would be covered by the centers if the overlap was not taken into consideration:[29]

$$\Theta(t_d) = 1 - \exp(-S_e) \qquad (2)$$

with $\Theta(t_d)$ representing the film coverage. In the case of hexagonal grains:

$$S_e = N_0 * 1.5\sqrt{3} * a^2 * t_d^2 \qquad (3)$$

N_0 is the density of growth center.

With A-GaN and the deposition conditions defined in Figure 1b,c captions, N_0 is equal to 9 μm^{-2} in average. The *a* and *b* values are 0.14 and 0.66 μm h^{-1}, respectively. The crystal growth is strongly anisotopic. It is

(29) The Southampton Electrochemistry Group. *Instrumental Methods in Electrochemistry*; John Wiley: New York, 1988; Chapter 9, Electrocrystallisation, p 283.

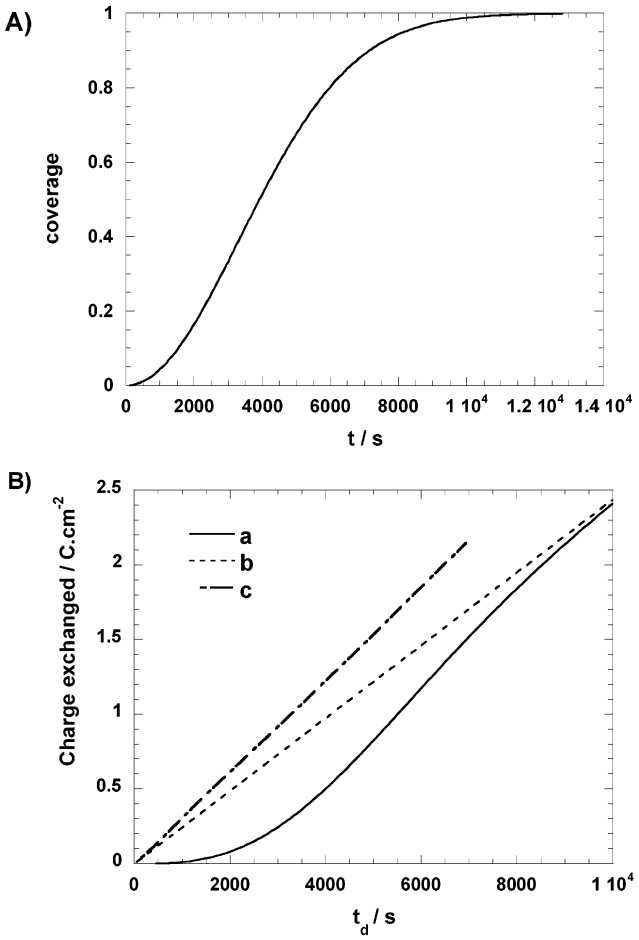

Figure 8. (A) Theoretical variation of the ZnO film coverage with time determined in the case of A-GaN, 27% O_2, $E_d = -1.4$ V; (B) variation with time of the charge involved in film formation: (a) calculated curve assuming a three-dimensional growth of the nuclei; (b) same curve calculated in the case of a layer by layer mechanism; (c) experimental curve (integration of Figure 2 curve b).

approximately five times faster on the (0001) plane than on the $(10\bar{1}0)$ and $(01\bar{1}0)$ planes. The shape of each hexagon is elongated. Accordingly, each plane growth rate is under the control of the kinetics of the surface reactions. The plane reactivity is related to the orientation of the coordination tetrahedron at the interface.[30] The polar (0001) plane, which contains only corners of the coordination tetrahedron, is reported as the most reactive.

Figure 8A presents the theoretical curve of the film coverage as a function of the deposition time calculated from eqs 2 and 3. The figure clearly shows that full merging occurs after a long polarization time of more than 2 h. We can read on the figure that the zinc oxide layer coverage is 53% in Figure 1b and 89% in Figure 1c.

The volume of the deposited film is given by

$$V(t) = \Theta(t) * b * t_d \qquad (4)$$

According to the two-electron process described in reaction 1, the charge exchanged for film formation is related to the film volume by

$$Q(t) = 2*F*(d/M)*V(t_d) \qquad (5)$$

with F representing the Faraday constant (96500 $C \cdot mol^{-1}$), d being the zinc oxide density (5.6 $g \cdot cm^{-3}$), and M representing the molar mass of zinc oxide (81.4 $g \cdot mol^{-1}$).

The variation of the charge consumed for zinc oxide electrocrystallization calculated from the three-dimensional model, described by eqs 2−5, is reported in Figure 8B as Curve a. In the same figure, we have also displayed the charge calculated for a layer-by-layer model ($Q(t_d) = 2*F*(d/M)b*t_d$, Curve b) and the Curve c is the experimental charge exchanged during the electrolysis (integration of Figure 2, Curve a).

During the first 2000 s, only a very small fraction of the charge is involved in ZnO formation, and the deposition efficiency is poor. This can be explained by the fact that only the hydroxide ions produced by reaction 1a in the vicinity of a nucleation center give rise to deposit formation, whereas those produced in GaN regions distant from a ZnO nucleus diffuse toward the bulk solution and are lost for the synthesis. At very large deposition time, when the film coverage is close to 1, curves a and b are superimposed and the growth becomes uni-dimensional, perpendicular to the substrate. The slope ratio between the curves b and c gives the deposition efficiency during the one-dimensional growth which is equal to ca. 80%. The behavior of electrogenerated hydroxide ions during the three-dimensional growth period is summarized schematically in Figure 9.

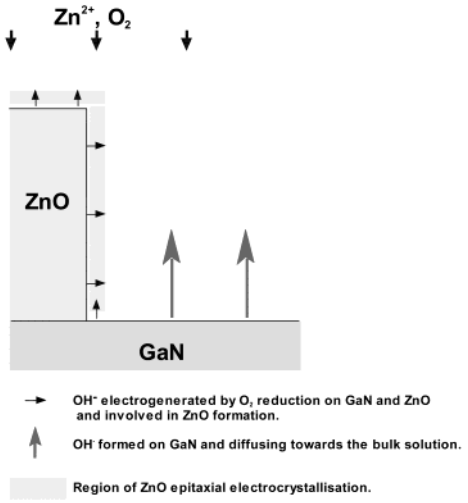

Figure 9. Schematic representation of behavior of the electrogenerated hydroxide ions during the three-dimensional epitaxial growth.

The useful GaN surface treatment consists of dipping the substrate in a basic solution of aqueous ammonia. This should greatly promote the formation of hydroxyl groups on the surface and a part of GaN may be transformed into $Ga(OH)_3$ which is more active for oxygen reduction (the surface treatment result in an onset of the cathodic current density) and allows anchoring of the zinc oxide seeds onto the surface. The

(30) Li, W. J.; Shi, E. W.; Zhong, W. Z.; Yin, Z. W. *J. Cryst. Growth* **1999**, *203*, 186.

study clearly shows that the fine control of the formation of this layer may allow the monitoring of high-quality epilayers.

Conclusions

The nucleation and growth process of epitaxial ZnO electrocrystallized onto GaN has been studied in detail and modeled. The deposit morphology can be tailored from epitaxial dots to fully covering flat single-crystal films. The film is formed by grain merging after a long enough polarization time. No critical thickness effect has been observed and the epitaxial films can be more than one micrometer thick. We have shown that the nucleation is a very fast process and that the growth rate depends on the zinc oxide facet. It is five times faster on the {0001} planes than on the $\{10\bar{1}0\}$ and $\{01\bar{1}0\}$ family of planes. A simple model based on the Avrami Theorem shows that if the deposition efficiency is low at the beginning of the deposition, it progressively increases and reaches a plateau (equal to 80% with 27% O_2, a deposition potential of −1.4 V, and A-GaN substrate) once the three-dimensional growth period is finished.

We have compared the nucleation and the structural properties of epitaxial ZnO deposited onto GaN(0001) of two different qualities. Substrates presenting a defect density of 100 μm^{-2} and a mosaicity of 0.47° can be directly used without any pre-deposition treatment. The nucleation seems to start directly on surface defects. The resulting ZnO presents a mosaicity of 0.74° and a texture of 0.60°. However, GaN of higher quality (0.25−0.28° of mosaicity and 1 defect per μm^{-2}) cannot be used directly. We have observed that a 20−35 min chemical pretreatment in hot ammonia was efficient to allow the nucleation process. This chemical treatment gives rise to epitaxial deposits of lower quality in terms of mosaicity (fwhm between 1.67° and 1.91°), with a similar texture of 0.58°. We suggest the formation of a buffer thin layer of chemically modified GaN has a detrimental effect on the epitaxial relationship of ZnO with the substrate. These results show the importance of monitoring the substrate surface chemistry in order to promote OH^- generation and zinc oxide nucleation. The chemically induced substrate surface modifications are currently under further investigation.

CM020349G